Submitted to Journal
of Physical Chemistry

UCRL-20508
Preprint

c.2

DYNAMICS OF THE REACTIONS OF O_2^+ WITH H_2 AND D_2

M. H. Chiang, E. A. Gislason, B. H. Mahan,
C. W. Tsao, and A. S. Werner

January 1971

AEC Contract No. W-7405-eng-48

TWO-WEEK LOAN COPY

*This is a Library Circulating Copy
which may be borrowed for two weeks.
For a personal retention copy, call
Tech. Info. Division, Ext. 5545*

UCRL-20508 c.2

LAWRENCE RADIATION LABORATORY
UNIVERSITY of CALIFORNIA BERKELEY

DISCLAIMER

This document was prepared as an account of work sponsored by the United States Government. While this document is believed to contain correct information, neither the United States Government nor any agency thereof, nor the Regents of the University of California, nor any of their employees, makes any warranty, express or implied, or assumes any legal responsibility for the accuracy, completeness, or usefulness of any information, apparatus, product, or process disclosed, or represents that its use would not infringe privately owned rights. Reference herein to any specific commercial product, process, or service by its trade name, trademark, manufacturer, or otherwise, does not necessarily constitute or imply its endorsement, recommendation, or favoring by the United States Government or any agency thereof, or the Regents of the University of California. The views and opinions of authors expressed herein do not necessarily state or reflect those of the United States Government or any agency thereof or the Regents of the University of California.

Dynamics of the Reactions of O_2^+ With H_2 and D_2

M. H. Chiang, E. A. Gislason, B. H. Mahan,
C. W. Tsao, and A. S. Werner.

Inorganic Materials Research Division of the Lawrence Radiation Laboratory and Department of Chemistry, University of California, Berkeley, California.

Velocity vector distributions of the ionic products of the reactions $O_2^+(H_2,H)HO_2^+$, $O_2^+(H_2,OH)OH^+$, $O_2^+(H_2,O)H_2O^+$, $O_2^+(D_2,O)O^+$ as well as nonreactively scattered O_2^+ are reported for several initial relative kinetic energies of collision. For relative energies below 5 eV, the distributions of HO_2^+, OH^+, and H_2O^+ all show the forward-backward symmetry characteristic of a reaction mechanism which involves a persistent $H_2O_2^+$ collision complex. At higher initial relative energies, a transition to direct or impulsive reaction mechanism is observed. The O^+ product appears to be formed by a direct interaction mechanism at all energies at which it can be detected. The distributions of nonreactively scattered O_2^+ give evidence of both direct and complex scattering mechanisms. The behavior of the system is qualitatively consistent with predictions based on the known major features of the potential energy surface.

As reported in a series of recent publications,[1-4] this laboratory has investigated the dynamics of exothermic ion-molecule reactions in which a hydrogen or deuterium atom is transferred from the neutral target to the projectile ion such as Ar^+ or N_2^+. These reactions typically have large total cross sections, and the product ion velocity vector distributions in the center-of-mass system are strongly peaked in the original direction of the projectile ion beam. Rebound scattering of the product through barycentric angles as large as 180° is observed, and at initial relative energies above 4 eV, the contribution of this process is nearly as great as that of the small angle stripping process.

It seemed clear to us that an entirely different dynamical behavior might be found in endothermic ion-molecule reactions, particularly those in which the intermediate collision complex had a substantial potential energy minimum with respect to both reactants and products. The reactions

$$O_2^+(^2\Pi_g) + H_2 \rightarrow HO_2^+ + H \qquad \Delta H^o = 1.96 \text{ eV} \qquad (1)$$

$$\rightarrow OH^+ + OH \qquad \Delta H^o = 1.87 \qquad (2)$$

$$\rightarrow H_2O^+ + O \qquad \Delta H^o = 0.66 \qquad (3)$$

$$\rightarrow O^+ + H_2O \qquad \Delta H^o = 1.66 \qquad (4)$$

all satisfy these criteria, and can be conveniently explored with our ion beam apparatus. Accordingly, we undertook investigations of Reactions (1-4) and certain of their isotopic

variations, and report the results here. Preliminary communications on this system have already appeared.[5,6]

EXPERIMENT

The instrument used in this work has been described in detail previously.[2] It consists of a magnetic mass spectrometer for preparation of a collimated beam of primary ions of known energy, a scattering cell to contain the target gas, and an ion detection train made up of an electrostatic energy analyzer, a quadrupole mass spectrometer, and an ion counter. The detector components and the exit slit of the scattering cell are mounted on a rotatable lid, which permits the intensity of scattered ions to be measured at various angles and energies.

The primary ions were extracted from a microwave discharge through oxygen. Because of the low electron temperature (~5 eV) that is characteristic of these discharges, relatively few electrons have energies greatly in excess of 10 eV. Consequently, most of the ionization is produced by electrons which have energies which are not much greater than the ionization energy of the gas (12.2 eV), and the number of metastable excited ions such as $O_2^+(^4\Pi_u)$, which requires 16 eV to be produced, is much smaller in a microwave discharge than in a conventional 50 eV electron impact source.

Beam attenuation experiments of the type described by Turner et al.,[7] showed that the momentum analyzed O_2^+ beam contained less than 3% excited metastable ions. The vibrational excitation of the ions in the $^2\Pi_g$ ground state of O_2^+ is not

known, but Franck-Condon factors[8] suggest that most molecules are in the excited vibrational levels 1-5, with the average vibrational energy being approximately 0.6 eV. This is probably a realistic upper limit to the vibrational energy of O_2^+, since we estimate that the ions undergo at least one and perhaps as many as 50 collisions with O_2 in this relatively high pressure (20-50 μ) source before being extracted from the plasma. Measurements of the kinetic energy threshold for the reaction and dissociation of O_2^+ also suggested that the ions have approximately 0.6 eV internal energy.

Our experimental results are presented in the form of contour maps[2] of the specific intensity, $\overline{I}(\theta,u)$, or the intensity of ions per unit velocity space volume normalized to unit beam strength, scattering gas density, and collision volume. A polar coordinate system is used, with the radial coordinate u representing the speed of the ion relative to the center-of-mass of the target-projectile system, and the angular coordinate θ measured with respect to the original direction of the projectile ion beam. The specific intensity is normalized so that

$$\overline{\sigma} = 2\Pi \int_0^{\Pi} \sin\theta d\theta \int_0^{\infty} u^2 \, \overline{I}(\theta,u)du$$

is always proportional to the true total cross section σ.

While the original experimental points are not usually shown on the intensity contour maps, each map is generated from 10-20 scans of the laboratory energy and angular distributions, in each of which 10-20 intensity measurements are

made. For the more complicated intensity distributions, even more data are collected. All of the contour maps show circles of constant Q, the difference between the final and initial relative translational energies. Assuming ground state reactants we can write

$$Q = \frac{1}{2}\mu'(g')^2 - \frac{1}{2}\mu g^2 = -\Delta E_o^o - U' + U$$

where ΔE_o^o is the energy change for reactants and products in their ground states, and U and U' are the internal excitation energies of reactants and products, respectively.

RESULTS AND DISCUSSION

In analyzing the experimental results, it is helpful to consult Table I, which lists the enthalpy changes[9] for forming various products and the intermediate $H_2O_2^+$ from ground state O_2^+ and H_2. It is clear that all possible reactions are endothermic, and that the collision complex $H_2O_2^+$ represents a substantial potential energy minimum. It must be borne in mind, however, that while the energies of the separated products and reactants are known, there is very little information available about potential energy barriers which may lie between reactants and various products. Such barriers of course could profoundly affect the reaction dynamics. The appearance potentials of the various ions formed from H_2O_2 by electron impact do indicate the magnitudes of potential barriers which lie between $H_2O_2^+$ and its various decomposition products.

Accordingly, the appearance potentials measured by Foner and Hudson[10] are listed in Table I.

We now shall present the results and discussion successively for each channel proceeding approximately in increasing order of complication.

A. $O_2^+ + D_2 \rightarrow O^+ + O + D_2$

Figure 1 shows the intensity distribution of O^+ produced by the collisional dissociation of O_2^+ by D_2 at an initial relative energy of 11.2 eV. The distribution is asymmetric about the $\pm 90°$ line in the barycentric system. This clearly shows that the dissociation occurs by a direct or short-lived collisional interaction. In addition, the O^+ intensity peaks at a velocity which is very nearly equal to the velocity of the original O_2^+ projectile. This indicates that in the most probable collision process, one of the atoms of the projectile is only slightly disturbed by the dissociation, and proceeds on as O^+ at nearly the velocity of the original projectile.

In interpreting Fig. 1 and other maps of the specific intensity, it must be kept in mind that the contribution of scattering out of the plane of the beam and detector is not included. To take account of the products scattered out-of-plane, one could multiply each specific intensity by $\sin\theta$, where θ is the barycentric scattering angle. This would remove the intensity maximum from $\theta = 0$ and place it at some greater angle in the forward scattering hemisphere. In a strict sense, inclusion of the $\sin\theta$ factor is inappropriate and can be somewhat misleading if the apparatus resolution is relatively poor,

as is true for the case at hand. Consequently, we omit this factor in the maps presented here. However, a map which includes the sinθ factor still leads to the conclusion that the free O^+ ion has, in the dissociation process, been subject to the finite but relatively small forces which product forward scattering.

Figure 2 shows that when the D_2 target is replaced by He, a very similar distribution of O^+ results. In another paper,[11] we have reported extensive measurements of the dissociation of O_2^+, NO^+, N_2^+, and N_2O^+ by collision with helium. Our conclusion from that work was that these dissociations occur principally by a version of the stripping process in which the target atom collides with one of the atoms of the projectile and breaks the projectile bond either adiabatically or through excitation to a weakly bound or slightly repulsive electronic state. The other projectile atom, which is ultimately detected as O^+ is thus subject only to relatively weak forces and proceeds at nearly its original velocity throughout the dissociation. The great similarity between Figs. 1 and 2 suggests that the dissociation of O_2^+ by collision with D_2 proceeds in a similar manner.

In an experiment in which O_2^+ collided with D_2 at 5.55 eV relative energy, no O^+ was observed, despite the fact that only 1.6 eV is required to form D_2O and O^+. Thus, aside from our observation that the total cross section for dissociation of O_2^+ by D_2 is larger than for dissociation by He at the same

relative energy, we have no evidence that either the existence of a long-lived $D_2O_2^+$ complex or the possibility of forming D_2O product has any influence on the dynamics of the dissociation process. It seems of considerable interest that the dissociation occurs by a direct interaction with D_2, for we shall see that the other reaction channels in this system are strongly affected by the potential energy minimum which corresponds to $D_2O_2^+$.

B. $O_2^+ + D_2 \rightarrow O_2^+ + (D_2)$

The nonreactive scattering of O_2^+ by D_2 depends in an interesting manner on the scattering angle of the relative energy of collision. Figure 3 shows that when the initial relative energy is 3.91 eV, there is considerable small angle scattering which is elastic within experimental uncertainty. As the angle increases past 60°, the scattered intensity greatly decreases and the intensity maxima lie in regions for which Q, the difference between the final and initial relative kinetic energies, is increasingly negative. Thus the scattering which produces this outer ridge becomes progressively more inelastic as the scattering angle increases. The monotonic evolution of this ridge from high intensity elastic scattering at small angles to lower intensity inelastic scattering at large angles suggests that the entire ridge is caused by direct interaction processes which occur in moderate to large impact parameter collisions.

This direct interaction mechanism seems to be considerably attenuated at angles greater than 135°, where the intensity ridge disappears. Apparently, the small impact parameter collisions which would be expected to contribute to scattering in this very large angle region in fact lead to chemical reaction or inelastic scattering with a broad distribution of internal excitations. There is also a substantial scattered intensity of O_2^+ at or near to the center of mass velocity. This indicates that a considerable fraction of the collisions are very inelastic, and leave the O_2^+ and D_2 sharing up to 3.91 eV as internal excitation energy.

In analyzing scattering from a reactive target, it is often very enlightening to compare it to the scattering of the same projectile from an inert target of the same mass. In Fig. 4 we show the intensity of O_2^+ scattered from a helium target at 5.55 eV initial relative energy. At angles greater than 90° the scattering becomes increasingly inelastic as the angle increases. At 180°, the most probable value of Q is -1.5 eV. In another paper[12] we have reported more extensive measurements of inelastic scattering in this and other such nonreactive systems, and have successfully interpreted the scattering in terms of classical theories of vibrational excitation. Thus Fig. 4 represents the vibrational excitation of O_2^+ that can be expected from collisions in which the interaction is of the direct, nonchemical type.

Figure 4 should be compared with Fig. 5, which shows O_2^+ scattered from D_2 at 5.57 eV initial relative energy. In the

O_2^+-D_2 system, virtually all the O_2^+ at large angles has been scattered very inelastically. In fact, the back-scattering of greatest intensity lies very close to the center-of-mass velocity, and therefore involves collisions in which nearly 5.57 eV is shared as intenal excitation of O_2^+ and D_2, or is used to dissociate D_2.

The fact that the inelasticities found for the O_2^+-D_2 and O_2^+-He systems differ greatly is consistent with the existence of a collision complex $D_2O_2^+$ in which the atoms interact through strong chemical forces. However, the data for nonreactive scattering does not, by itself, prove that this complex is necessarily long-lived. For example,[2,4] in the systems N_2^+-D_2 and Ar^+-D_2 which involve reaction by direct, short-lived interaction, the N_2^+ that does not react is scattered very inelastically, while the unreacted Ar^+ shows only very small inelasticity. On the basis of our experience, it appears that the existence of strong chemical interactions does not necessarily lead to nonreactive collisions of great inelasticity, but that inelasticity substantially greater than that predicted by classical vibrational energy transfer theory indicates either electronic excitation or strong coupling of the nuclear motions through valence forces.

When the initial relative energy of O_2^+ and D_2 exceeds 6 eV, the intensity distribution of the scattered O_2^+ shows a secondary maximum in the small angle inelastic region. Figure 6 shows that when the initial relative energy is 11.1 eV, this feature has developed into a fairly well-defined intensity

ridge (see the ellipse of intensity 50 K). The asymmetry of this feature about the $\pm 90°$ line makes it seem very unlikely that it is connected with the existence of a long-lived collision complex. It also seems unlikely that the cause of this ridge is vibrational excitation of the collision partners by direct interaction, since we should expect large, rather than small angle scattering, and a broad, rather than well-defined range of inelasticities from such a process. Much the same arguement eliminates simple adiabatic one-step or knock-on collisional dissociation of D_2 as a likely origin of this scattering.

The inelastic feature in Fig. 6 resembles the one which we found[2] in the nonreactive scattering of N_2^+ by D_2. From a determination of the energy threshold for the N_2^+-D_2 inelastic process, we concluded that it arose principally from the excitation of D_2 to its lowest $^3\Sigma_u$ state by grazing collisions. A similar finding was made[3] in the N_2^+-CD_4 system, and was rationalized in a similar manner. The same explanation may in fact be valid for the inelastic feature in the O_2^+-D_2 system. However, the existence in this system of large amounts of elastic and inelastic scattering which cannot be unequivocally separated from the inelastic ridge makes it impossible for us to determine a partial cross section and energy threshold for this feature, and thereby to test the electronic excitation hypothesis thoroughly.

Another possible explanation for the inelastic peak is that it arises from the dissociation of DO_2^+ molecules which are formed by a stripping type process[2] and have internal energies in excess of the 2.6 eV dissociation energy of the $D-O_2^+$ bond. It can be easily demonstrated that the internal energy U' of DO_2^+ formed by the spectator stripping process is given by

$$U' = E_a - \Delta E_o^o$$

where E_a is the energy of the projectile O_2^+ relative to the <u>atom</u> abstracted. The excitation energy of any DO_2^+ formed by spectator stripping thus rises linearly with the projectile energy until U' equals 2.6 eV. At this point (a relative energy of 8.6 eV for $O_2^+-D_2$) any DO_2^+ formed by spectator stripping becomes unstable with respect to dissociation to O_2^+ and D. The resulting O_2^+ should have a velocity approximately equal to that calculated for DO_2^+ formed by spectator stripping.

The well-defined inelastic peak or ridge in Fig. 6 first makes its appearance at approximately 8 eV initial relative energy, quite close to the value of 8.6 eV predicted from the spectator stripping. These observations strongly suggest that, at least at relative energies above 8 eV, some or all of the small angle inelastic feature may represent collisional dissociation of D_2 by O_2^+ through the spectator stripping mechanism. However, careful examination of Figs. 3 and 5 shows that at energies below 8.6 eV, there is important, if not

particularly well defined inelastic scattering in the small angle region. Experiments with H_2 targets also show this feature. Since the dissociative stripping mechanism cannot operate in this low energy regime, we are inclined to attribute these small angle inelastic features to electronic excitation of H_2 to the $^3\Sigma_u$ state. Thus there is evidence for dissociation of D_2 both by electronic excitation and the dissociative stripping process, and it seems likely that both occur at relative collision energies above 8.6 eV.

C. $O_2^+ + D_2 \rightarrow DO_2^+ + D$

In a preliminary communication,[5] we have briefly summarized our findings for this reaction. At low relative energies of collision (<5 eV) the DO_2^+ product (or HO_2^+ from O_2^+-H_2 collisions) has a very nearly isotropic specific intensity distribution in the center-of-mass system. This is illustrated in Fig. 7, which is typical of several of the maps which we have determined in this low energy regime. The isotropy indicates the occurrence of a long-lived collision complex of relatively small total angular momentum and large internal energy per vibrational and rotational mode. The small total cross section ($\sim$2 Å^2) and large bonding energy (2.4 eV) with respect to D_2 and O_2^+ are consistent with such a deduction.

Another factor that may contribute substantially to the isotropy is the rotational angular momentum of the O_2^+ drawn from the microwave discharge. While the temperature of the

discharged gas was not measured, it could easily be 400°K, which would correspond to a most probable J of 9 for O_2^+. The plane of rotation, and thus the angular momentum vector of O_2^+ is randomly oriented with respect to the O_2^+-D_2 relative velocity vector. Therefore, rotation of O_2^+ is a factor which tends to randomize the relation between the initial relative velocity vector and the total angular momentum vector or orientation of the complex, and thus tends to produce an isotropic product distribution.

In investigations of O_2^+-HD collisions,[5,6] we have found that at low initial relative energies, both HO_2^+ and DO_2^+ are distributed isotropically in the center of mass system, and that the intensity of DO_2^+ exceeds that of HO_2^+ by as much as a factor of eight. These results constitute further evidence that the $O_2^+(D_2,D)DO_2^+$ reaction proceeds by a long-lived collision complex at these lower relative kinetic energies. The prevalence of DO_2^+ over HO_2^+ is the opposite of the isotope effect that we found for reactions which proceed by a direct interaction mechanism. However, because DO_2^+ has a lower zero point energy and higher density of states than does HO_2^+, the isotope effect expected from the statistical decay of a long-lived HDO_2^+ collision complex should favor formation of DO_2^+ over HO_2^+, as is observed in the experiments.

In an attempt to determine whether there is an activation energy barrier for the reaction which exceeds the endothermicity of 1.96 eV, we studied the $O_2^+(H_2,H)HO_2^+$ reaction down to initial relative energies of 1.47 eV. While the relative reaction

cross section decreased as the relative energy was lowered past 2.0 eV, considerable product intensity remained even when the nominal initial relative energy was as low as 1.47 eV. In view of the uncertainty of ± 0.20 eV in the initial relative energy due to target gas motion and ion beam energy spread, and the estimated 0.6 eV vibrational excitation of the O_2^+, it is not surprising that a reaction threshold was not observed at 1.96 eV, nor even in the 1.47 eV experiment. Diminished beam intensities prevented significant experiments at lower energies. However, it seems clear that if there is an activation barrier for the $O_2^+(H_2,H)HO_2^+$ reaction, its height is not significantly in excess of 2.1 eV. These experiments also indicate that the barrier for <u>formation</u> of the $H_2O_2^+$ complex from O_2^+ and H_2 is not significantly greater than 2.1 eV. On the other hand, if all products are formed by decomposition of an $H_2O_2^+$ complex, the fact that significant products are formed at all suggests that the barrier for formation of the complex from reactants is not much lower than the endothermicity for formation of HO_2^+ or OH^+. If this were not so, most complexes would simply redissociate to reactants over the low barrier between reactants and complex. The picture that emerges then is that the barrier for formation of the $H_2O_2^+$ complex with a hydrogen peroxide structure from O_2^+ and H_2 is comparable in height to the energy plateau which represents HO_2^+ product formation.

Support for this conclusion is found in the work of Foner and Hudson[10] on the mass spectrometry of H_2O_2. These authors found that the appearance potential of O_2^+ and H_2 from H_2O_2 is 15.8 ± 0.5 eV, whereas the thermodynamic minimum energy required for this change is 13.42 eV. Therefore, $O_2^+ + H_2$ are formed from $H_2O_2^+$ with internal or kinetic energy amounting to 2.4 ± 0.5 eV. This means there is a 2.4 ± 0.5 eV barrier for forming $H_2O_2^+$ from O_2^+ and H_2, which is consistent with our earlier conclusion.

Figures 8, 9, and 10 show that as the initial relative kinetic energy is increased above 5 eV, the angular distribution of DO_2^+ loses its isotropy, and acquires an intensity maximum in the forward scattering region. The forward peaking increases in relative importance with increasing energy. These distributions of DO_2^+ found in high energy experiments are qualitatively similar but clearly broader than the product distributions from the $Ar^+(D_2,D)ArD^+$ and $N_2^+(D_2,D)N_2D^+$ reactions.[2,4] Thus the DO_2^+ distributions indicate that as the initial relative energy is increased, the lifetime of the $D_2O_2^+$ collision complex decreases to less than one full rotational period, and the reaction mechanism tends toward the direct or impulsive types of interaction.

The reaction $O_2^+(D_2,D)DO_2^+$ has recently been investigated by Ding and Henglein,[13] who determined the translational energy spectrum of DO_2^+ in the primary beam direction without angular intensity measurements. The O_2^+ was prepared by impact of 100 eV electrons in a conventional mass spectrometer source,

and contained substantial amounts of the metastable $^4\Pi_u$ state of O_2^+. Ding and Henglein were able to separate the effects of this excited state from the reactions of ground state O_2^+, and showed that below 4 eV relative energy the reaction of ground state O_2^+ produced DO_2^+ moving at the velocity of the center-of-mass, as would be expected from the decay of a long-lived complex. When the initial relative energy was above 5 eV, the maximum intensity of DO_2^+ fell at velocities greater than that of the center-of-mass, and with increasing initial energy eventually reached the value expected from the ideal stripping process. A threshold for production of DO_2^+ from ground state O_2^+ was found at approximately 1.9 eV relative energy. In view of our failure to observe a sharp threshold for this reaction, this finding of Ding and Henglein is somewhat surprising. In other respects, however, the two investigations are nicely consistent in the regions in which they overlap.

The qualitative reason for the change in reaction mechanism with increasing relative kinetic energy is clear from unimolecular reaction rate theory. The lifetime of the collision complex is determined by its total internal energy as compared to the minimum amount needed to decompose, and by the total number of internal modes which share the total energy. The simplest expression for the lifetime τ of the collision complex is that derived from the Rice-Ramsperger-Kassel theory,[14] which treats the energized molecule as a

collection of s degenerate oscillators of frequency ν:

$$\tau = (1/\nu)[E/(E-E_o)]^{s-1}$$

Here E is the total internal energy and E_o is the minimum energy needed for decomposition. Because of failures of the assumptions of the model, this expression can give lifetimes which are incorrect by orders of magnitude, and therefore should not be used for quantitative calculations of τ. However, the formula does correctly indicate the important quantitative trends that τ decreases as the internal energy E increases, and the molecular complexity decreases.

In order to calculate the lifetime of the $D_2O_2^+$ collision complex quantitatively, we used the RRKM theory[14] of unimolecular decomposition. The vibration frequencies for $D_2O_2^+$ were estimated by analogy to those of D_2O_2, with allowance for the increased O-O bond strength in $D_2O_2^+$. The vibrational energy level densities were evaluated by the method of Whitten and Rabinowitch.[15] The total internal energy of the complex was set equal to the sum of the initial relative kinetic energy and the binding energy of reactants, plus 0.6 eV to allow for the vibrational energy of O_2^+. The maximum impact parameter for reaction was evaluated from the approximate cross section for DO_2^+ formation, and from this, the reduced mass, and the initial relative velocity, the maximum angular momentum was calculated.

In Table II we give a comparison between the lifetime of the complex with respect to dissociation to DO_2^+ and D as calculated using RRKM theory, and the "experimental" lifetime. The possibility of the complex decomposing to $O_2^+ + D_2$, $DO_2^+ + D$, $OD^+ + OD$, and $D_2O^+ + O$ was included in the calculation. The experimental lifetime was estimated from the experimental intensity ratio of forward to back scattered DO_2^+ using the fall-off function for osculating complexes given by Fisk, McDonald, and Herschbach.[16] In calculating the rotational frequencies used in constructing Table II, we have assumed that $D_2O_2^+$ has approximately the same geometry as D_2O_2. It is, therefore, nearly a prolate symmetric top with one small moment of inertia I_A corresponding to the rotation of the deuterium atoms around the O-O axis, and two large and nearly equal moments of inertia I_B and I_C corresponding to the tumbling of the oxygen atoms.

One sees from Table II that in the experiment at 5.5 eV relative energy, the $D_2O_2^+$ complex had a maximum experimental lifetime of approximately one rotational period. For the same experiment, RRKM theory predicts a lifetime of 0.8 rotations about the B or C axes, or 5 rotations with the same angular momentum about the unique A axis. Since the reaction occurs in effect by ejection of a D atom from the $D_2O_2^+$ complex, it would appear that the significant motion in determining the forward-backward symmetry of the product angular distribution is the high frequency rotation about the unique axis. That is,

the circulation of the deuterium atoms about the O-O axis destroys any memory of the direction from which O_2^+ came much more rapidly than does the precession or tumbling of the O-O axis about the total angular momentum vector. If this argument were valid, then we would be forced to conclude that RRKM theory overestimates the lifetime of the $D_2O_2^+$ complex by approximately a factor of six.

There is reason to expect that complexes will tend to have only a small fraction of their total angular momentum present as rotation about the unique axis. The assumption of statistical equilibrium corresponding to a rotational temperature T_r leads to a distribution function P(K) for the quantum number K for rotation about the unique axis which is given by[17]

$$P(K) = \exp\left(-\frac{1}{2} K^2/K_a^2\right)$$

where

$$K_a = \left|kT_r I_r/\hbar^2\right|^{1/2}$$

and

$$I_r = I_B I_A/(I_B - I_A)$$

Thus high values of K are not favored, and the rotational angular momentum will tend to reside in the low frequency tumbling motions of the O-O axis.

It can also be argued that complexes which do have large amounts of their angular momentum present as rotation about the unique axis will not dissociate to the products DO_2^+ and D.

If we treat the separation of the products as a two-body problem with a (negative) potential energy $\phi(r)$, then rotation of the complex creates a maximum in the effective potential V_{eff} for separation of the products:

$$V_{eff} = L^2\hbar^2/(2\mu r^2) + \phi(r)$$

Here $L\hbar$ is the orbital angular momentum of the separating products, μ is their reduced mass, and r is their separation. This two-body approximation is appropriate if the maximum in the effective potential comes at a value of r large enough so that the internal motions of the fragments are essentially decoupled from their motion along the reaction coordinate.

The maximum which occurs in the effective potential energy curve can be viewed as a barrier which complexes must cross in order to become products. Alternatively, and perhaps more satisfactorily, it can be pictured as an ejection potential which supplies final relative kinetic energy to product particles that have crossed it. The height of this barrier (with respect to products) is given by

$$V_B = (L\hbar)^4/(C_4)(4\mu)^2 \qquad (1)$$

when ϕ is the ion-induced dipole potential $-C_4/r^4$.

We see from Eq. (1) that large amounts of angular momentum L coming from rotation of the complex combined with small reduced masses for the products can create a high barrier in the exit channel. In the case at hand, the barrier height may be as much as 1 eV above the asymptotic product potential energy.

Products would be expected to have this much relative translational energy, and therefore to lie well away from the center of mass velocity. This is not found experimentally. In fact, the intensities of Fig. 8 have maximum values on the Q = -4.75 eV circle, which corresponds to the minimum possible final translational energy consistent with product stability. It appears, therefore, that in the dissociation of $D_2O_2^+$ to DO_2^+ and D, the angular momentum of the complex must be converted to angular momentum of rotation of the DO_2^+ entity, rather than appear as orbital angular momentum (and thus product translational energy) of DO_2^+ and D.

In order to explain the high internal excitation of the DO_2^+ product, we must find a mechanism by which the total angular momentum of the complex ($\sim$150 $\hbar$) is converted to rotation of DO_2^+ rather than to orbital motion of D and DO_2^+. This conversion requires that angle dependent forces act between the D and DO_2^+ fragments as they begin to separate to products. Since $D_2O_2^+$ in the hydrogen peroxide structure would have an equilibrium OOD angle of approximately 105°, separation of D from DO_2^+ in a direction approximately parallel to the O-O axis would produce torques which could result in excitation of rotation of DO_2^+. This mode of separation might be particularly favored in $D_2O_2^+$ complexes in which most angular momentum was contained in the tumbling around the B and C axes. Indeed, this type of rotation would seem to be required if the incipient orbital rotation of D about DO_2 were to be converted efficiently to rotation of DO_2^+.

In contrast, separation of D from DO_2^+ in a direction more nearly perpendicular to the O-O axis would seem to be an inefficient way to convert orbital momentum to product rotation. There are, of course, angle dependent forces which are responsible for the internal rotation barrier in hydrogen peroxide, but these are relatively weak compared to the forces required to bend chemical bonds. Thus, it seems that rotation of the complex about the unique axis cannot be readily converted to rotation of the DO_2^+ fragment.

In view of the foregoing considerations, we feel that there will tend to be relatively few $D_2O_2^+$ complexes which have substantial amounts (150 $\hbar$) of angular momentum present as rotation about the unique axis. Those which do apparently do not dissociate to D and DO_2^+ because of the high effective potential energy barrier and the difficulty of converting this angular momentum into product rotation. Thus the high frequency rotation about the unique axis of the complex is not effective in maintaining the isotropy of the DO_2^+ angular distribution as the collision energy is increased. The predictions of the RRKM theory for the lifetime of the complex should therefore be compared with the period for rotation about the B and C axes of $D_2O_2^+$.

The data in Table II show that the RRKM calculation of the lifetime of the $D_2O_2^+$ complex is consistent with experimental observations of the symmetry of the DO_2^+ angular distribution, provided that rotation of the complex about the B and C axes of the prolate top determines this symmetry. There is, however, considerable uncertainty in the molecular parameters and total

angular momentum of the complex, and this fact tends to make the agreement between calculated and experimental lifetimes less significant as a test of RRKM theory.

It is also worth noting that it may not be entirely valid to test a statistical model like the RRKM theory in an energy region where we expect to see the beginning of the failure of the statistical picture of rapid distribution of energy among all internal modes. In the experiment done at 5.5 eV relative energy, the calculated lifetime of the complex is long enough to allow only 3-10 vibrations in the various modes of $D_2O_2^+$. Even considering the strong anharmonic coupling, this would seem to be nearly the minimum number of vibrations necessary for complete randomization of the internal energy. Failure to distribute the total energy over the entire molecule would result in a lifetime of the complex shorter than that calculated from RRKM theory.

We should also remark that while RRKM theory gives a satisfactory indication of the lifetime of the complex $D_2O_2^+$, the relative yields of products depart noticeably from what one would calculate using this theory. Relative to the OD^+ formed the amount of DO_2^+ exceeds, and the amount of D_2O^+ is less than expected on the basis of the simplest application of RRKM theory. This suggests that some DO_2^+ may be formed by direct interaction at all energies, or that complexes with other than the hydrogen peroxide geometry may be involved. These points will be explored in a subsequent paper on the isotope effects and product velocity distributions for this system.

D. $O_2^+ + D_2 \rightarrow OD^+ + OD$

Several maps of the intensity of OD^+ or OH^+ from the reaction of O_2^+ with D_2 and H_2 were obtained. Two of these are shown in Figs. 11 and 12. It is clear that at both low and high initial relative energies the distribution of OH^+ or OD^+ shows considerable symmetry about the ±90° line in the center-of-mass coordinate system. However, this reaction represents a situation in which such symmetry cannot be taken as proof of the existence of a long-lived collision complex. The products OD^+ and OD are very nearly identical, and there is no reason to expect that even direct, impulsive interactions will lead to preferential scattering of OD^+ in either the forward or back direction, as long as the complex has, on the average, a symmetry that maintains the dynamical equivalence of the two oxygen atoms. On the other hand, if the potential energy surface were such as to allow reaction by a process such as

$$O_2^+ + D_2 \rightarrow OO^+ \cdots DD \rightarrow O + OD^+ + D$$

where in the linear collision complex the oxygen atoms are not equivalent, then there would be no reason to expect symmetry in the distribution of OD^+ at high energies.

It appears, therefore, that the observed highly symmetric distribution of OH^+ found in the experiment carried out at 2.93 eV relative energy (Fig. 11) implies <u>primarily</u> that the $H_2O_2^+$ collision complex has oxygen atoms which are dynamically equivalent. If, as seems highly likely, the OH^+ occurs as an

alternate decomposition product of the same collision complex that produces HO_2^+, then this complex not only has equivalent oxygen atoms, it is long-lived when its energy is low.

The high degree of symmetry of the OD^+ distribution found in the experiment performed with 8.3 eV relative energy (Fig. 12) also implies the prevalence of a collision mechanism in which the oxygen atoms are equivalent. While this equivalence could be the consequence of a long-lived complex of the hydrogen peroxide structure, it would seem impossible to maintain that a long-lived complex exists when the relative energy is so high. This is particularly true in view of the fact that formation of DO_2^+ occurs by a direct interaction at these high energies. We conclude, therefore, that OD^+ is formed at high energies by a direct, impulsive interaction in which the collision complex has geometries resembling the hydrogen peroxide structure. The small excess intensity of OD^+ in the small angle scattering region may be a consequence of formation of OD^+ by processes in which the oxygen atoms are not equivalent.

E. $O_2^+ + H_2 \rightarrow H_2O^+ + O$

This reaction is the least endothermic (0.66 eV) of all the reaction channels. It therefore would be expected to be the most important reactive process if products were formed at a rate proportional to their total phase space. Figure 13 shows that the angular distribution of H_2O^+ is isotropic even though the initial relative energy of collision (2.93 eV) is markedly greater than the endothermicity of reaction. Moreover, the

total intensity of H_2O^+ is less than those of OH^+ and HO_2^+ at the same relative collision energies. Both these facts suggest that the reaction path for decay of the $H_2O_2^+$ complex to H_2O^+ has in it a barrier which limits the available phase space of H_2O^+ and O, and prevents these products from being of greatest importance. On the other hand, Foner and Hudson[10] find that in the mass spectrum of H_2O_2, the products H_2O^+ and O appear at the thermodynamic threshold energy, and therefore are formed without significant internal or translational excitation. This finding refutes the postulate of an energy barrier in the H_2O^+ product channel.

It is also possible that the critical configuration of the $H_2O_2^+$ complex which leads to H_2O^+ is of highly constrained geometry. Such a "tight" complex would be consistent with both the small yield of H_2O^+, and the low appearance potential found by Foner and Hudson. A configuration in which $H_2O_2^+$ resembled a nonplanar formaldehyde molecule would have the necessary characteristics of high vibration frequencies in all but the reaction coordinate.

Figure 14 shows that even when the initial relative energy of collision is 5.9 eV, the distribution of H_2O^+ has considerable symmetry about the $\pm 90°$ line in the center-of-mass coordinate system. This persistence of the long-lived complex mechanism at higher energies is consistent with the low product yield, for if the critical configuration for forming H_2O^+ and O is of very low probability, it is likely that these products tend to be formed from complexes which have existed several rotational periods.

Figure 15 gives the velocity vector distribution of H_2O^+ formed from very energetic collisions (8.89 eV) of O_2^+ and H_2. The distribution is highly anisotropic, which indicates that H_2O^+ is formed by a direct interaction mechanism in this high energy regime. The velocity vector distribution is rather broad, and has a rather poorly defined maximum in the vicinity of the velocity H_2O^+ would have if it were formed by the spectator stripping mechanism. The latter would correspond to abstraction of O^+ from O_2^+ by H_2 with no momentum transfer to the free O atom. However, because of the extreme breadth of the H_2O^+ distribution, the term spectator stripping is a very poor description of the high energy mechanism. Moreover, since H_2O^+ can absorb only 5.7 eV as internal energy before dissociating, and most of the product in Fig. 15 lies in regions where Q is more negative than -5.7 eV, the oxygen atom formed with H_2O^+ must be electronically excited.

SUMMARY

In this paper we have demonstrated the existence of three reactions which proceed through a persistent collision complex at low initial relative kinetic energies. For the $O_2^+(D_2,D)DO_2^+$ and $O_2^+(H_2,O)H_2O^+$ reactions, we have shown that as the relative kinetic energy of collision is increased, the product angular distributions become asymmetric, and direct interaction mechanisms begin to dominate the dynamics. For the $O_2^+(D_2,OD)OD^+$ reaction, the product distribution remains quite symmetric even in the high energy regime, evidently because of the near identity

of the OD and OD^+ products, and dynamical equivalence of the oxygen atoms. These observations of the reaction dynamics can be qualitatively rationalized using thermodynamic and ion appearance potential data. The experimentally estimated lifetime of the collision complex formed in 5.5 eV relative energy collisions is in agreement with the prediction of the RRKM version of unimolecular reaction rate theory.

The nonreactive collisions between O_2^+ and D_2 lead to scattering patterns which are consistent with direct or potential scattering for small angles or large impact parameters, and with strongly interacting collision complexes for small impact parameter, large angle scattering. Collisions between O_2^+ and D_2 which produce O^+ appear to proceed only by a direct interaction, despite the influence of the persistent collision complex in the other product channels.

Acknowledgement: This work was supported by the U. S. Atomic Energy Commission. E.A.G. acknowledges a postdoctoral fellowship from the National Center for Pollution Control. B.H.M. wishes to express his appreciation of the early scientific guidance and continuing inspiration provided by Professor George B. Kistiakowsky, to whom this paper is dedicated.

References

1. W. R. Gentry, E. A. Gislason, Y. T. Lee, B. H. Mahan, and C. W. Tsao, Disc. Faraday Soc., **44**, 137 (1967).
2. W. R. Gentry, E. A. Gislason, B. H. Mahan, and C. W. Tsao, J. Chem. Phys., **49**, 3058 (1968).
3. E. A. Gislason, B. H. Mahan, C. W. Tsao, and A. S. Werner, J. Chem. Phys., **50**, 142 (1969).
4. M. Chiang, E. A. Gislason, B. H. Mahan, C. W. Tsao, and A. S. Werner, J. Chem. Phys., **52**, 2698 (1970).
5. E. A. Gislason, B. H. Mahan, C. W. Tsao, and A. S. Werner, J. Chem. Phys., **50**, 5418 (1969).
6. M. Chiang, E. A. Gislason, B. H. Mahan, C. W. Tsao, and A. S. Werner, J. Chem. Phys., **53**, 3752 (1970).
7. B. R. Turner, J. A. Rutherford, and D. M. J. Compton, J. Chem. Phys., **48**, 1602 (1968).
8. R. W. Nichols, J. Physics B (Proc. Phys. Soc.), **1**, 1192 (1968).
9. J. L. Franklin *et al.*, "Ionization Potentials, Appearance Potentials, and Heats of Formation of Gaseous Positive Ions," NSRDS-NBS 26 (1969).
10. S. N. Foner and R. L. Hudson, J. Chem. Phys., **36**, 2676 (1962).
11. M. H. Cheng, M. Chiang, E. A. Gislason, B. H. Mahan, C. W. Tsao, and A. S. Werner, J. Chem. Phys., **52**, 5518 (1970).

References (Continued)

12. M. H. Cheng, M. Chiang, E. A. Gislason, B. H. Mahan, C. W. Tsao, and A. S. Werner, J. Chem. Phys., 52, 6150 (1970).

13. A. Ding and A. Henglein, Ber. Bunsenges. Phys. Chem., 73, 562, (1969).

14. D. Bunker, "Theory of Elementary Gas Reaction Rates," Pergamon Press, New York, N.Y. (1966).

15. G. Whitten and B. S. Rabinovitch, J. Chem. Phys., 38, 2466 (1963).

16. G. A. Fisk, J. D. McDonald, and D. R. Herschbach, Disc. Faraday Soc., 44, 228 (1967).

17. W. B. Miller, S. A. Safron, and D. R. Herschbach, Disc. Faraday Soc., 44, 108 (1967).

Figure Captions

Fig. 1. A contour map of the specific intensity of O^+ from O_2^+-D_2 collisions at an initial relative energy of 11.2 eV. The radial coordinate is the speed of O^+ relative to the center of mass, and the angular coordinate is the center-of-mass system scattering angle, measured relative to the direction of the O_2^+ beam. The circle labelled Q = -6.5 is located assuming the D_2 and neutral O products retreat from O^+ with no kinetic energy relative to each other.

Fig. 2. A contour map of the specific intensity of O^+ from O_2^+-He collisions at 11.1 eV relative energy. The intensities are directly comparable to those in Fig. 1.

Fig. 3. A contour map of the specific intensity of O_2^+ scattered from D_2 at 3.91 eV relative energy. The circle marked Q = 0 is the locus of elastic scattering. Points closer to the origin correspond to negative Q values and hence inelastic scattering.

Fig. 4. A contour map of the specific intensity of the O_2^+ scattered by He at an initial relative energy of 5.55 eV. The small circles locate the actual intensity maxima found in each energy and angular sweep through the scattering pattern.

Fig. 5. The distribution of the specific intensity of O_2^+ scattered from D_2 at 5.57 eV relative energy. Note the smaller intensity near 180° and Q = 0, in comparison with Fig. 4.

Figure Captions (Continued)

Fig. 6. The distribution of the specific intensity of O_2^+ scattered from D_2 at 11.1 eV relative energy. The small circles locate intensity maxima as in Fig. 4. The circle marked Q = -6.48 is the approximate locus of scattered O_2^+ excited to nearly its dissociation limit (6.8 eV), while the Q = -9.9 eV circle locates O_2^+ which has excited D_2 vertically to its dissociative $^3\Sigma_u$ state. The cross at the inelastic peak is the velocity which DO_2^+ formed by the spectator stripping process would have.

Fig. 7. A contour map of the specific intensity of DO_2^+ from O_2^+-D_2 collisions at a relative energy of 3.86 eV. The circle marked Q = -2 eV is the locus of the maximum product velocity, assuming no motion of the target gas, no beam energy and angular spread, and infinite detector resolution.

Fig. 8. A contour map of the specific intensity of DO_2^+ from the O_2^+-D_2 reaction at 5.47 eV initial relative energy. The circles marked Q = -2 and -4.75 eV are, respectively, the velocity limits for products with the minimum and maximum allowable internal excitation. The cross marks the velocity of DO_2^+ formed by the spectator stripping process.

Figure Captions (Continued)

Fig. 9. A contour map of the specific intensity of DO_2^+ from the O_2^+-D_2 reaction at 8.34 eV initial relative energy. The cross locates the velocity of DO_2^+ formed by the spectator stripping process.

Fig. 10. A contour map of the specific intensity of DO_2^+ from the O_2^+-D_2 reaction. Note that the total intensity is small, and rather broadly distributed about the spectator stripping velocity, which is marked by a cross.

Fig. 11. A contour map of the specific intensity of OH^+ from O_2^+-H_2 collisions at 2.96 eV initial relative energy. The circle marked Q = -1.9 eV is the locus of OH^+ scattered without internal excitation in either product molecule.

Fig. 12. A contour map of the specific intensity of OD^+ from O_2^+-D_2 collisions at 8.38 eV relative energy. The circle marked Q = -6.6 eV corresponds to OD^+ and OD leaving the collision excited to the dissociation limits of their ground states. Scattering inside this circle must occur with electronic excitation of either product, or dissociation of OD.

Fig. 13. A contour map of the specific intensity of H_2O^+ formed by the O_2^+-H_2 reaction at 2.93 eV relative energy.

Figure Captions (Continued)

Fig. 14. A contour map of the specific intensity of H_2O^+ formed by the O_2^+-H_2 reaction at 5.88 eV initial relative energy. Product ions formed with zero velocity relative to the center of mass are unstable with respect to dissociation the H + OH^+ if the neutral O product is not electronically excited.

Fig. 15. A contour map of the specific intensity of H_2O^+ formed from O_2^+ and H_2 at 8.89 eV initial relative energy. Note the low intensity relative to that in Fig. 14. The circle marked Q = -8.1 eV passes through the broad intensity maximum. A Q value of -7.9 at θ = 180° corresponds to spectator stripping of the O^+ from O_2^+.

Table I. Enthalpies and Appearance Potentials

	ΔH_o^o (eV)[a]	V_{app} (eV)[b]
$H_2O_2^+$	-2.38	10.92 ± 0.05
$H + HO_2^+$	1.96	15.36 ± 0.05
$H + H + O_2^+$	4.47	
$OH^+ + OH$	1.87	15.35 ± 0.1
$OH^+ + O + H$	6.26	
$H_2O^+ + O$	0.66	14.09 ± 0.1
$H_2O + O^+$	1.66	
$H_2 + O + O^+$	6.78	
$H_2^+ + O_2$	3.37	
$H_2 + O_2^+$	0	15.8 ± 0.5

a. Enthalpy for forming specified products from O_2^+ and H_2.

b. Appearance potential for products from ionization of $H_2O_2^+$.

Table II. Lifetimes for the $D_2O_2^+$ Collision Complex

E_{rel} (eV)	τ_{calc} [a] (sec)	τ_{rot} [b] (sec)	τ_{rot} [c] $/\tau_{dis}$
3.86	4.7×10^{-13}	1.4×10^{-13}	≥ 5
5.47	1.1×10^{-13}	1.2×10^{-13}	~ 1
8.3	3.5×10^{-14}	0.9×10^{-13}	≤ 0.3

a. Calculated using RRKM theory with all channels.

b. Calculated assuming that the total orbital angular momentum appears as rotation about a nonunique axis.

c. Estimated using the fall-off function of ref. 16.

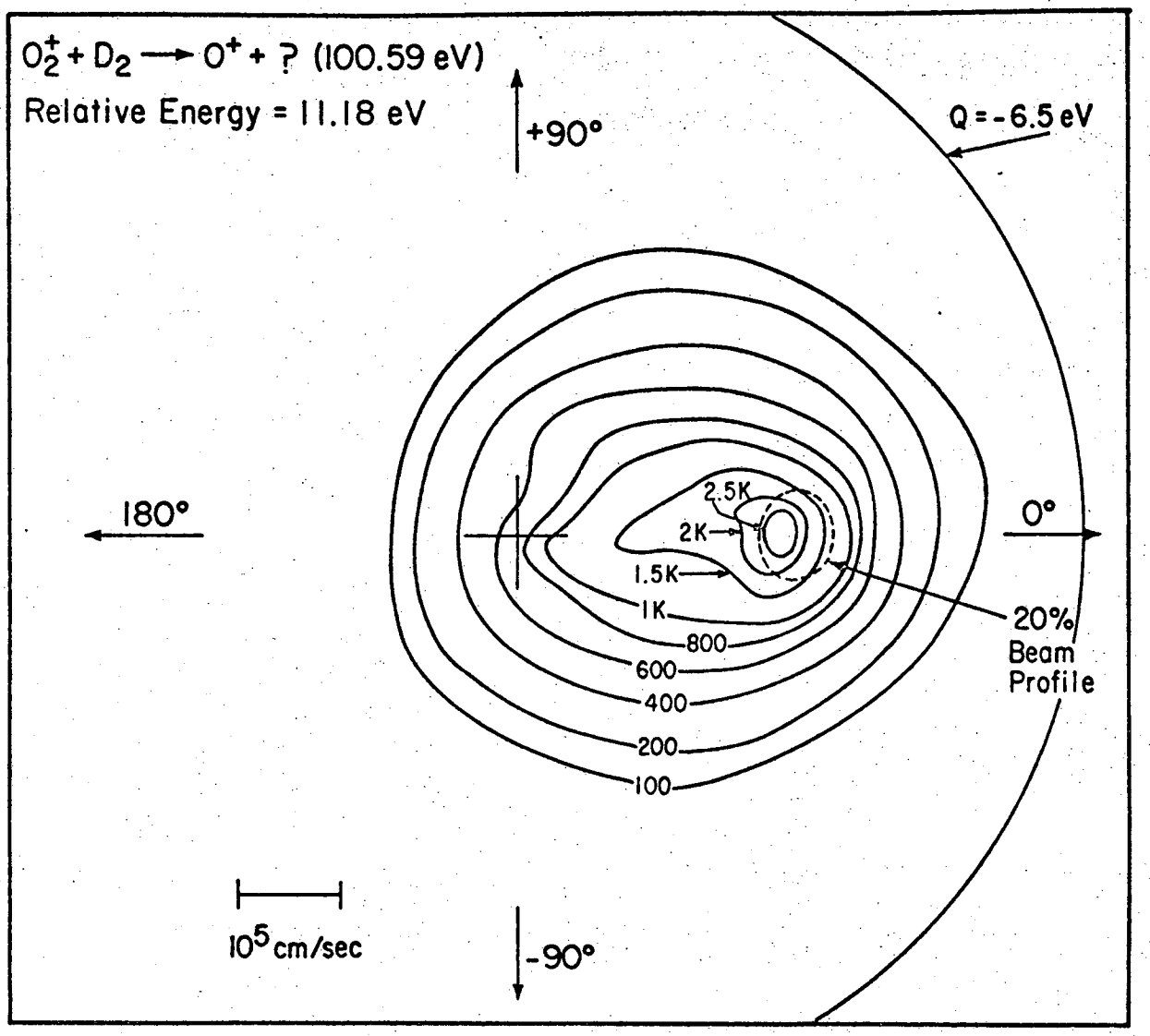

Fig. 1.

XBL 6912-6693

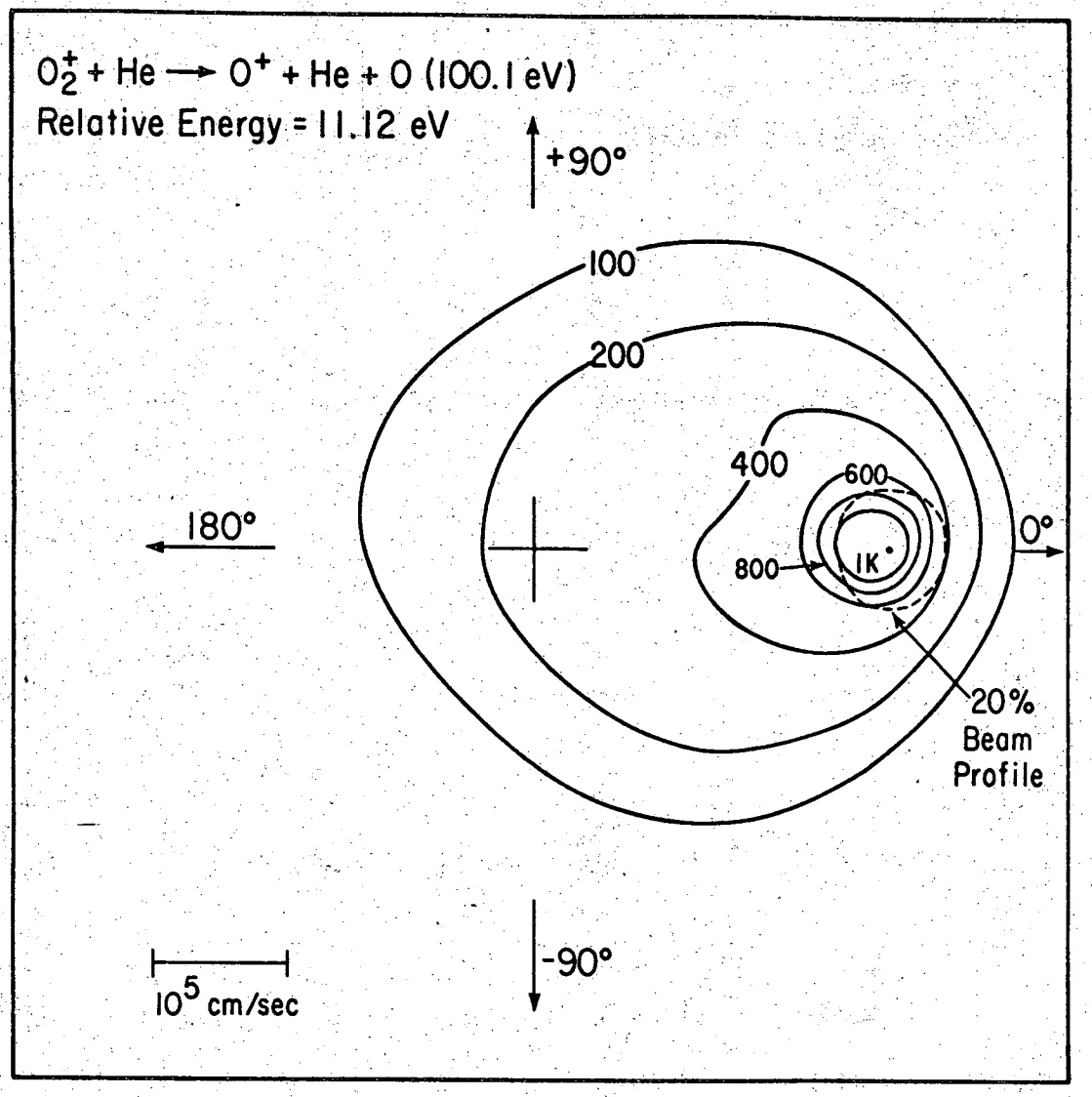

Fig. 2.

XBL 6912-6702

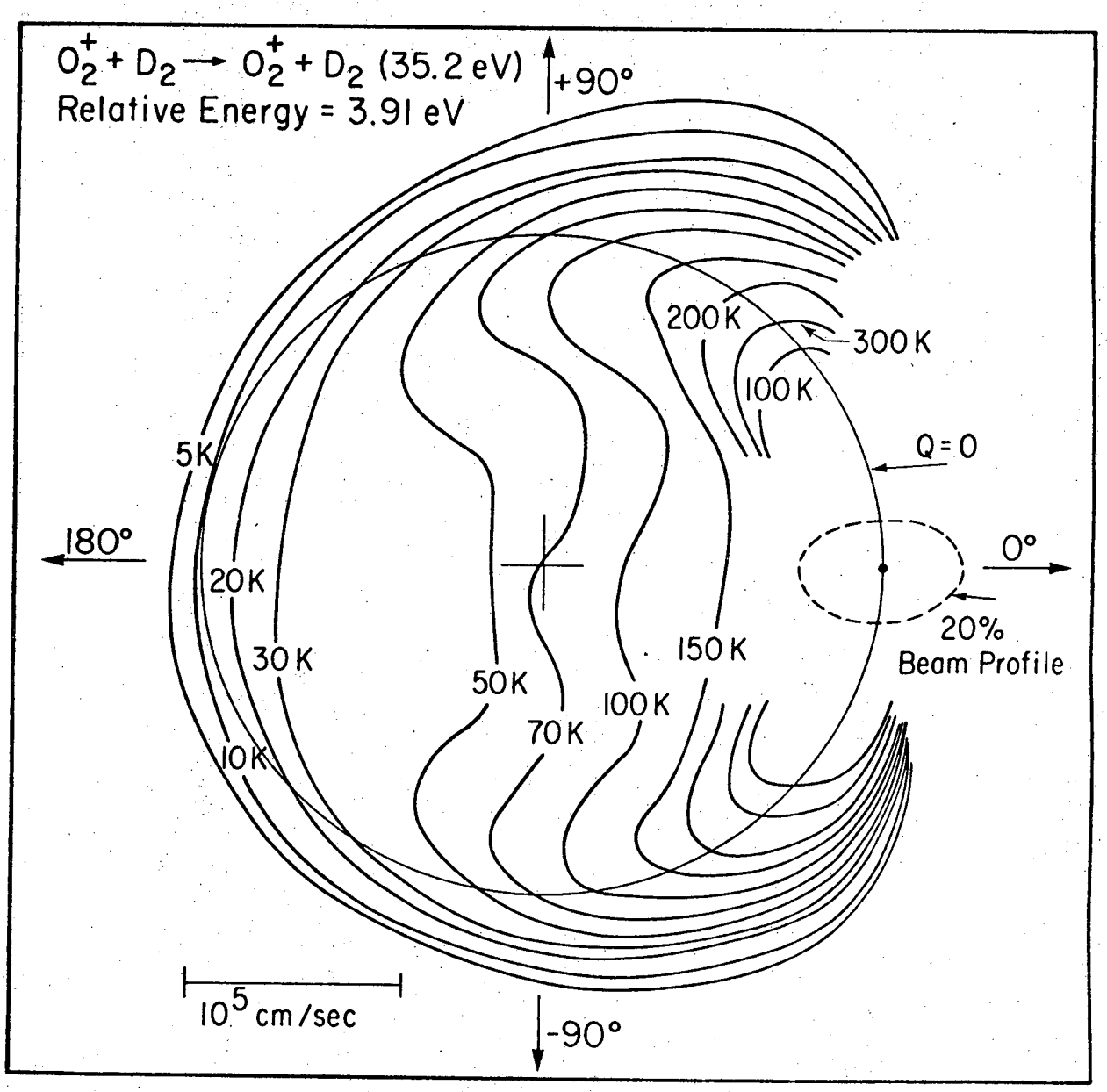
$O_2^+ + D_2 \rightarrow O_2^+ + D_2$ (35.2 eV)
Relative Energy = 3.91 eV
+90°
-90°
180°
0°
5K
10K
20K
30K
50K
70K
100K
150K
200K
300K
100K
Q=0
20%
Beam Profile
10^5 cm/sec

Fig. 3.

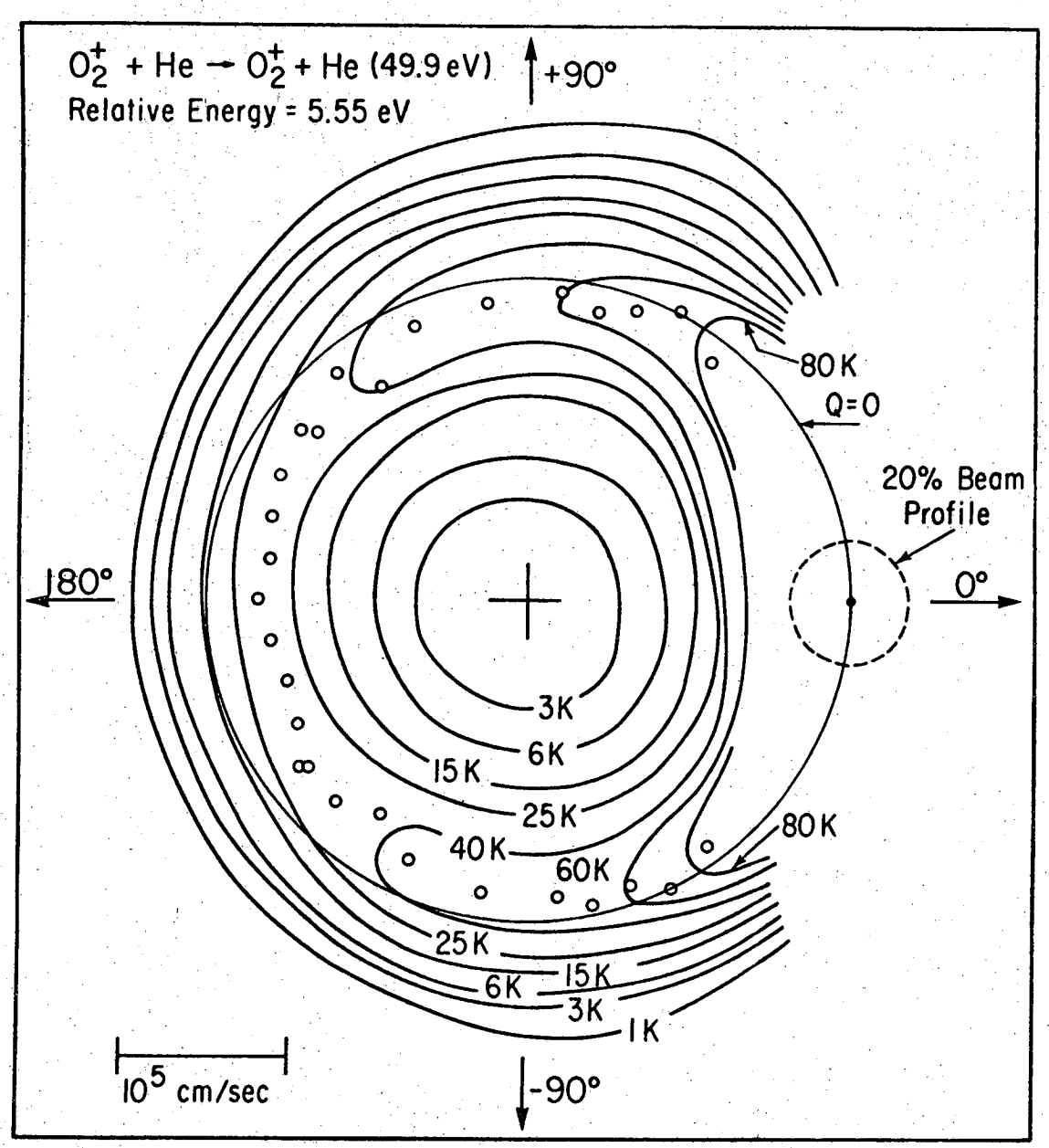
$O_2^+ + He \rightarrow O_2^+ + He$ (49.9 eV)
Relative Energy = 5.55 eV
+90°
-90°
180°
0°
80 K
Q=0
20% Beam Profile
3K
6K
15 K
25 K
40 K
60K
80 K
25 K
15 K
6K
3K
1 K
10^5 cm/sec

Fig. 4.

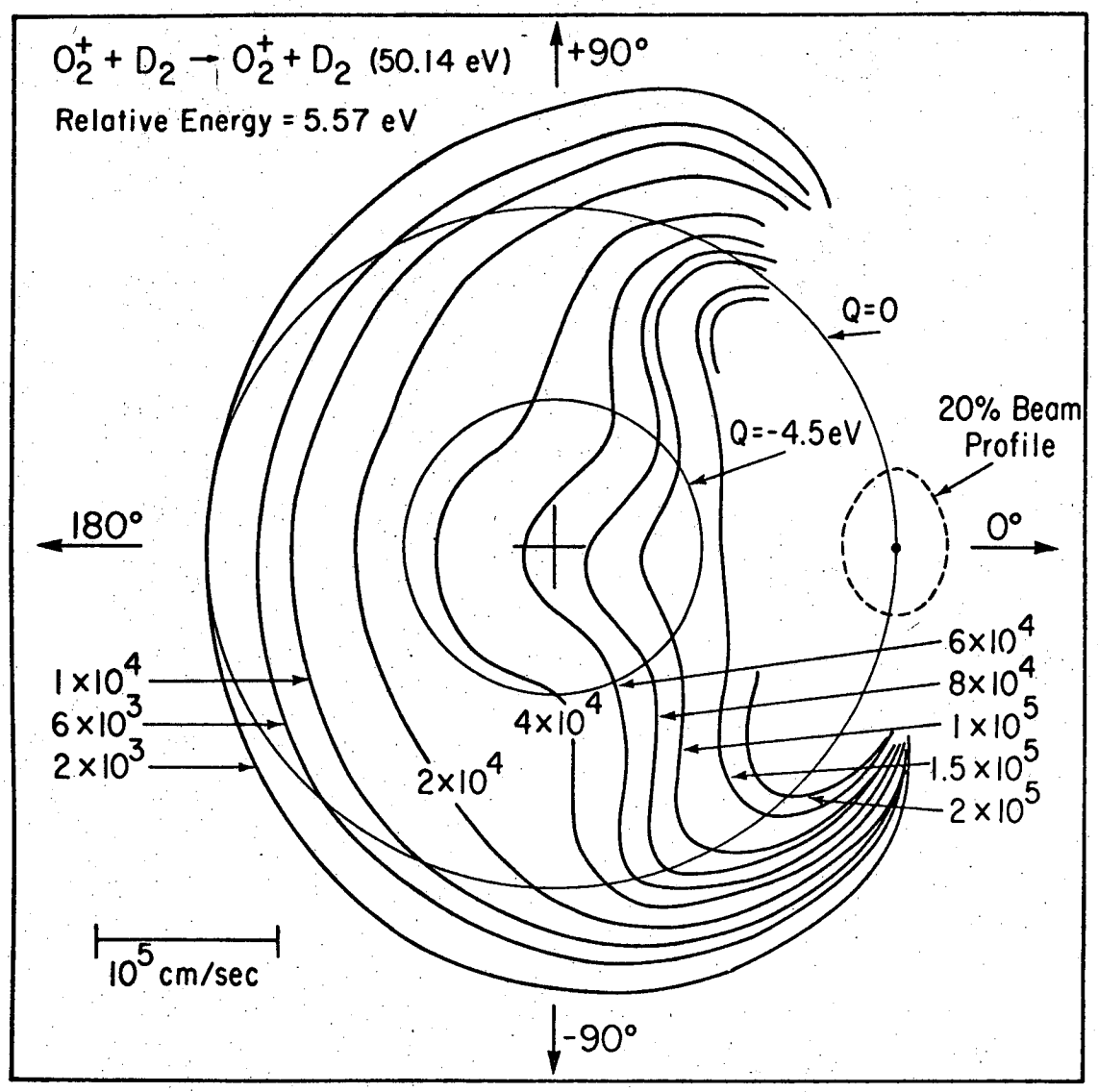

XBL 6912-6692

Fig. 5.

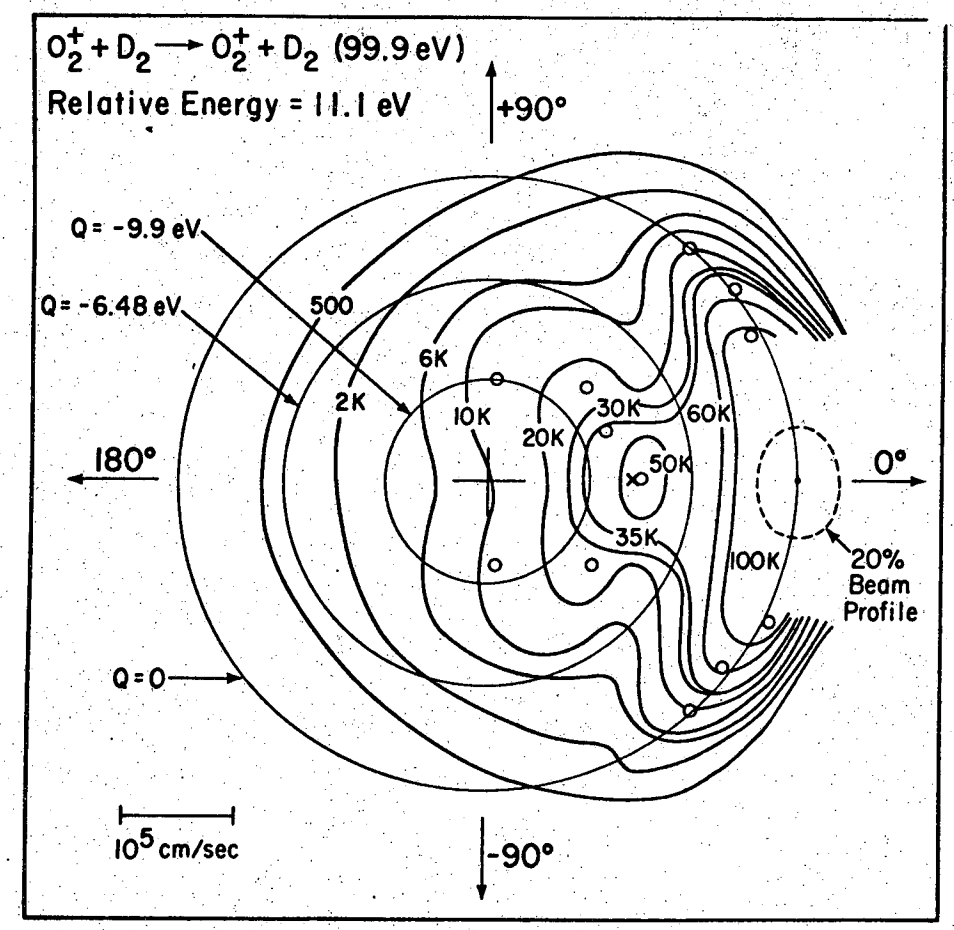
$O_2^+ + D_2 \rightarrow O_2^+ + D_2$ (99.9 eV)
Relative Energy = 11.1 eV
+90°
Q = -9.9 eV
Q = -6.48 eV
500
6K
2K
10K
20K
30K
60K
50K
35K
100K
180°
0°
20% Beam Profile
Q = 0
10^5 cm/sec
-90°

Fig. 6.

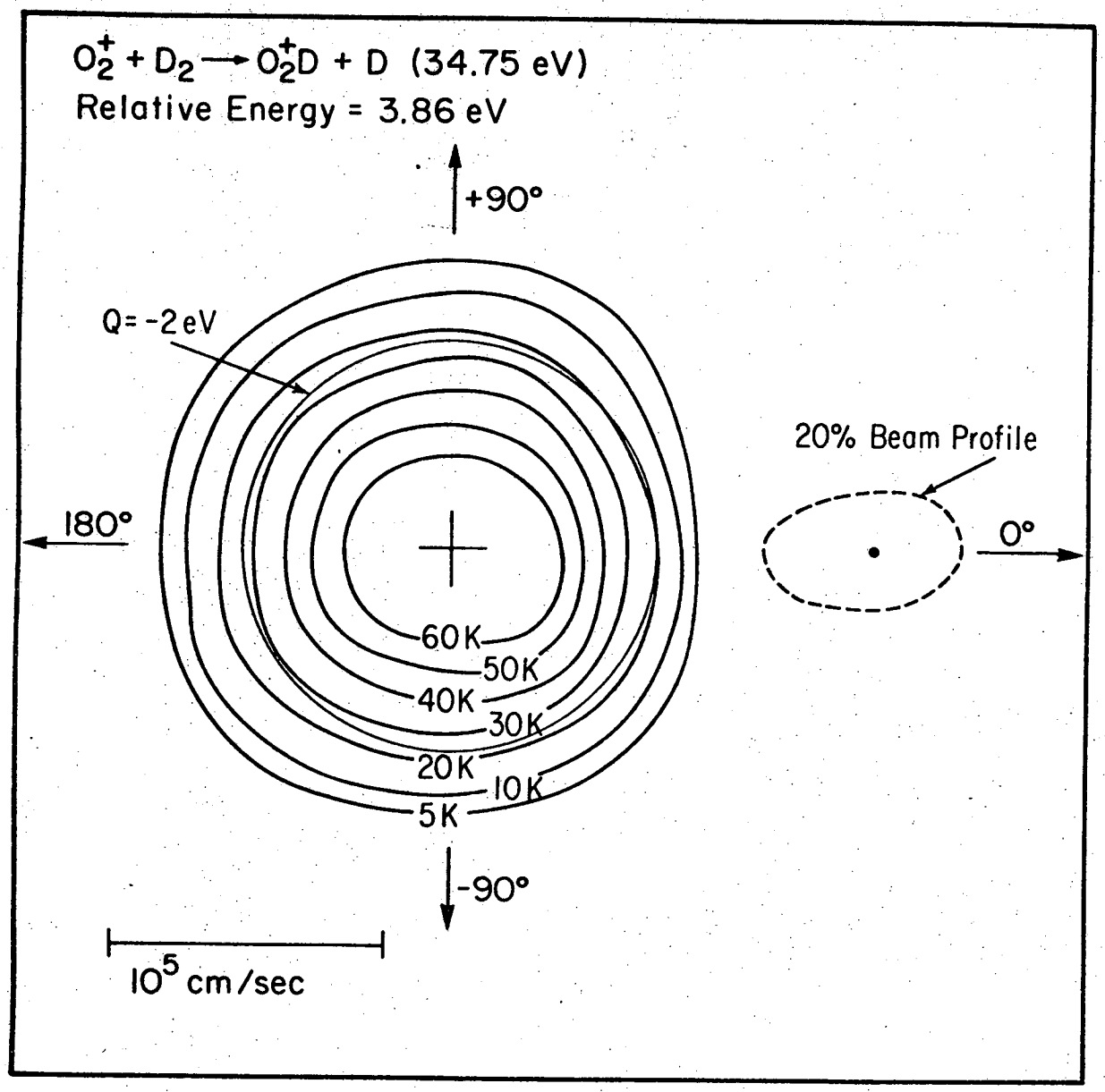

XBL 6912-6699

Fig. 7.

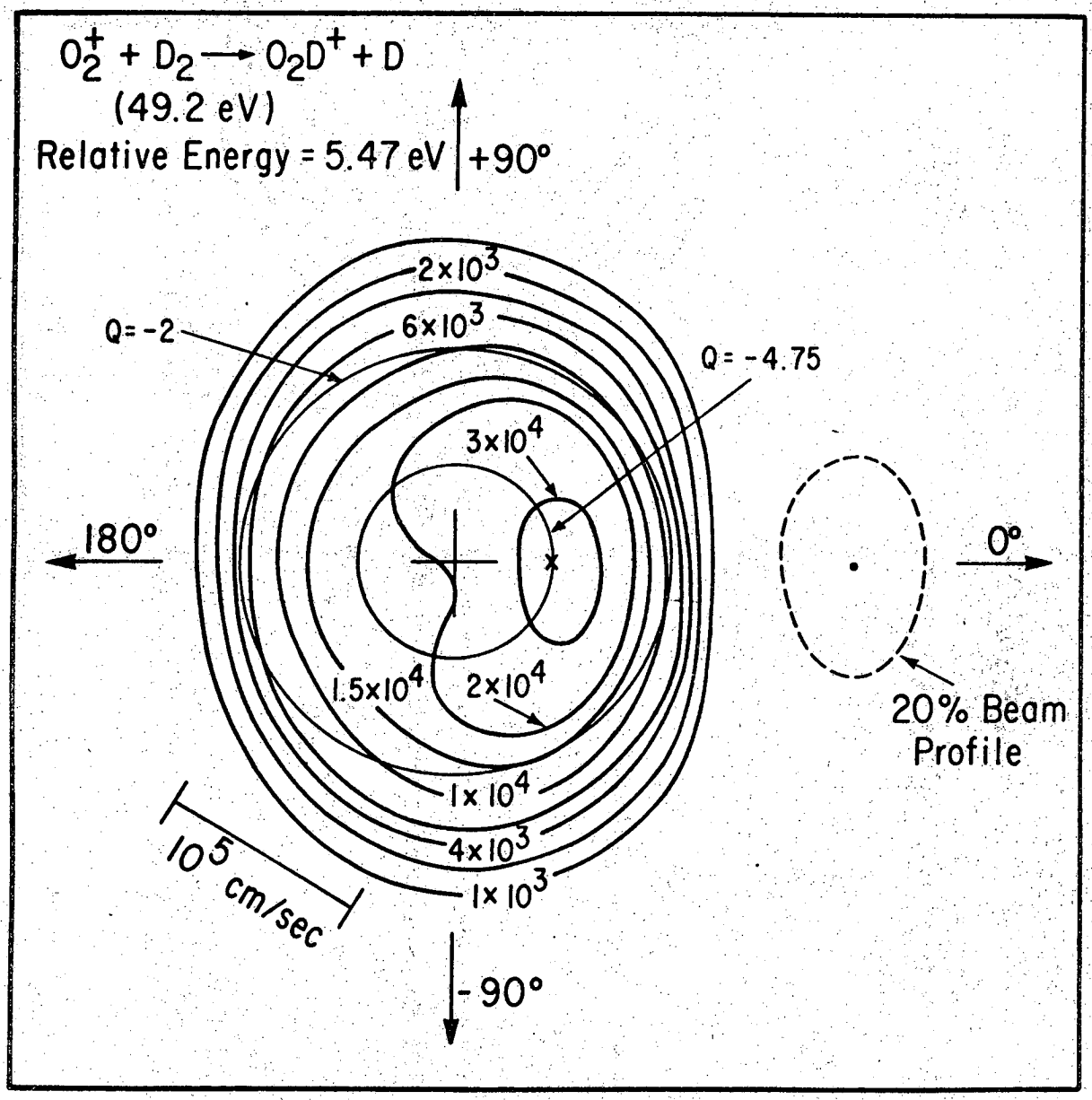
$O_2^+ + D_2 \rightarrow O_2D^+ + D$
(49.2 eV)
Relative Energy = 5.47 eV
+90°
2×10³
6×10³
Q = -2
Q = -4.75
3×10⁴
180°
0°
1.5×10⁴
2×10⁴
20% Beam Profile
1×10⁴
4×10³
1×10³
10⁵ cm/sec
-90°

Fig. 8.

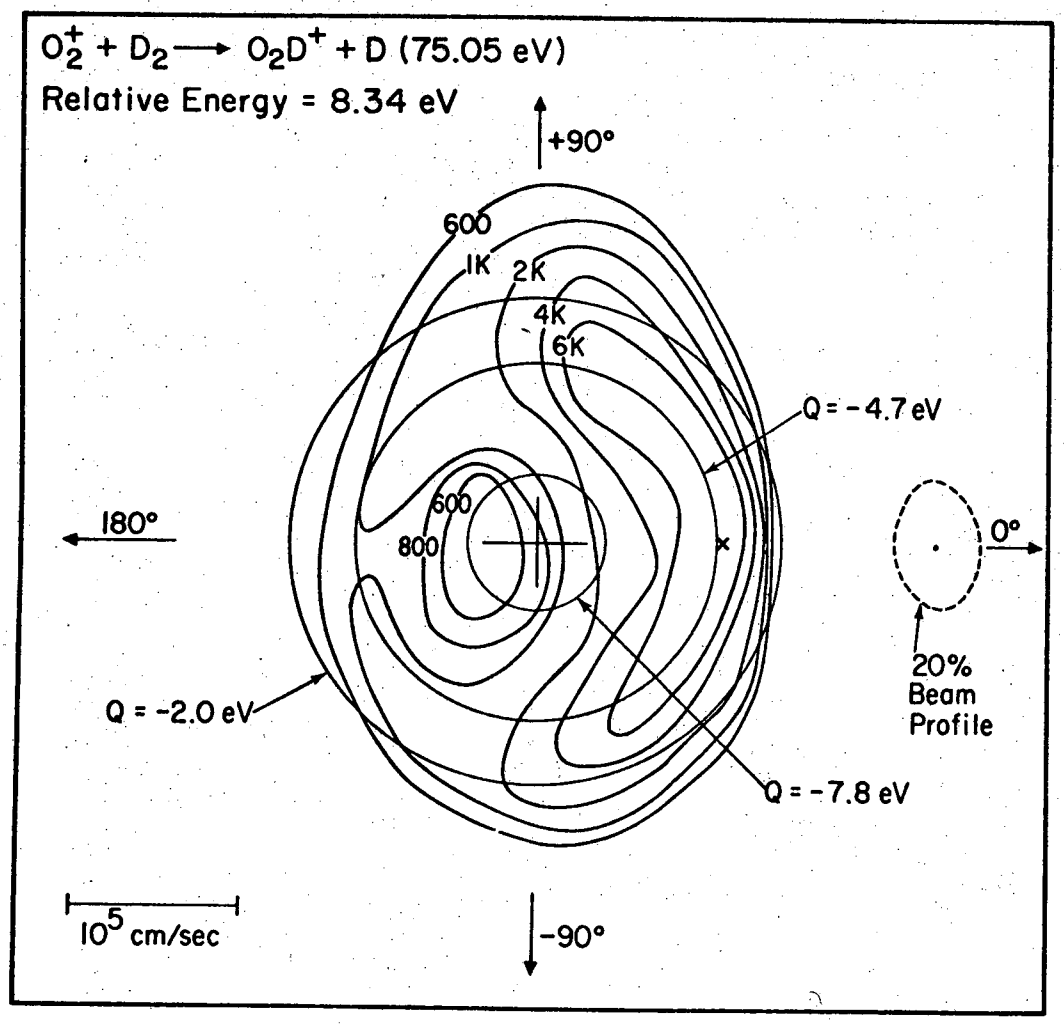
$O_2^+ + D_2 \longrightarrow O_2D^+ + D$ (75.05 eV)
Relative Energy = 8.34 eV
+90°
600
1K
2K
4K
6K
Q = -4.7 eV
180°
600
800
0°
20% Beam Profile
Q = -2.0 eV
Q = -7.8 eV
10^5 cm/sec
-90°

Fig. 9.

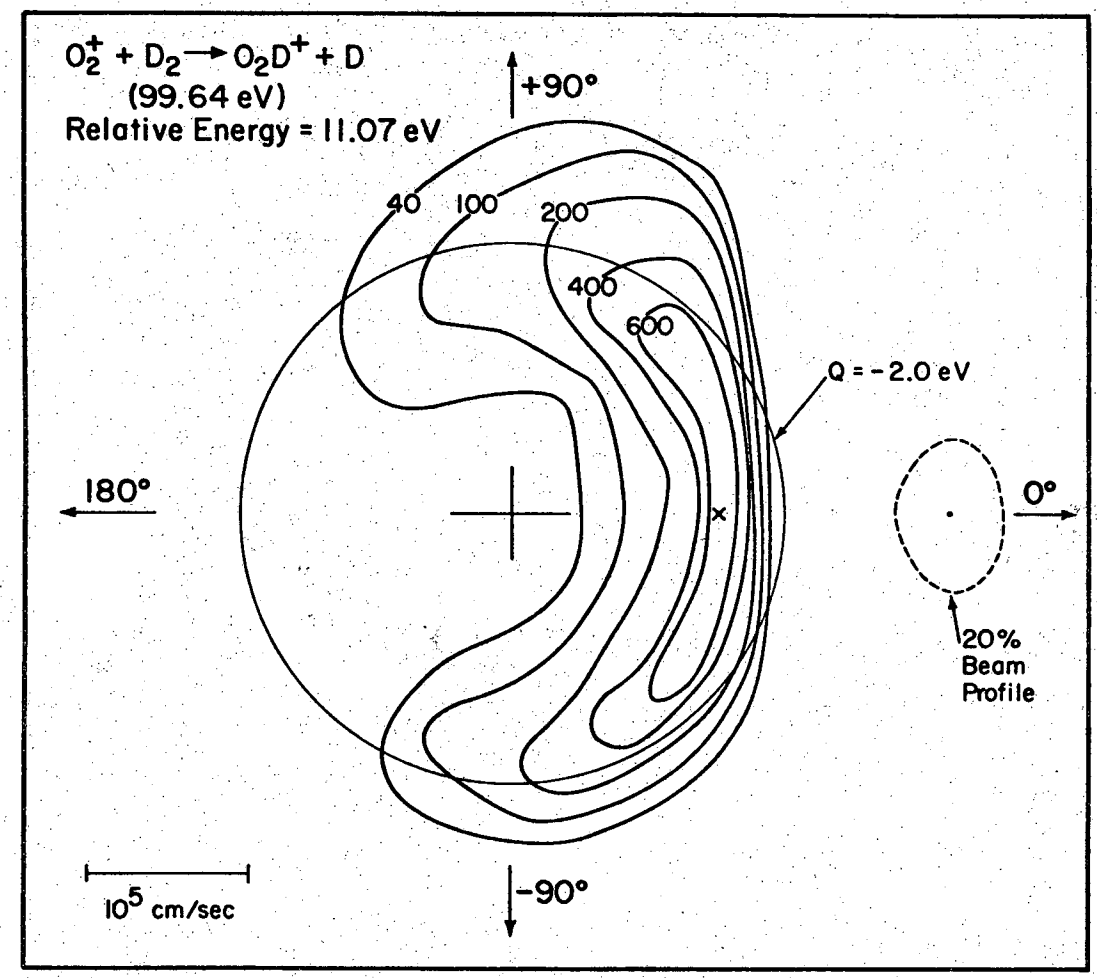

XBL 7012-7462

Fig. 10.

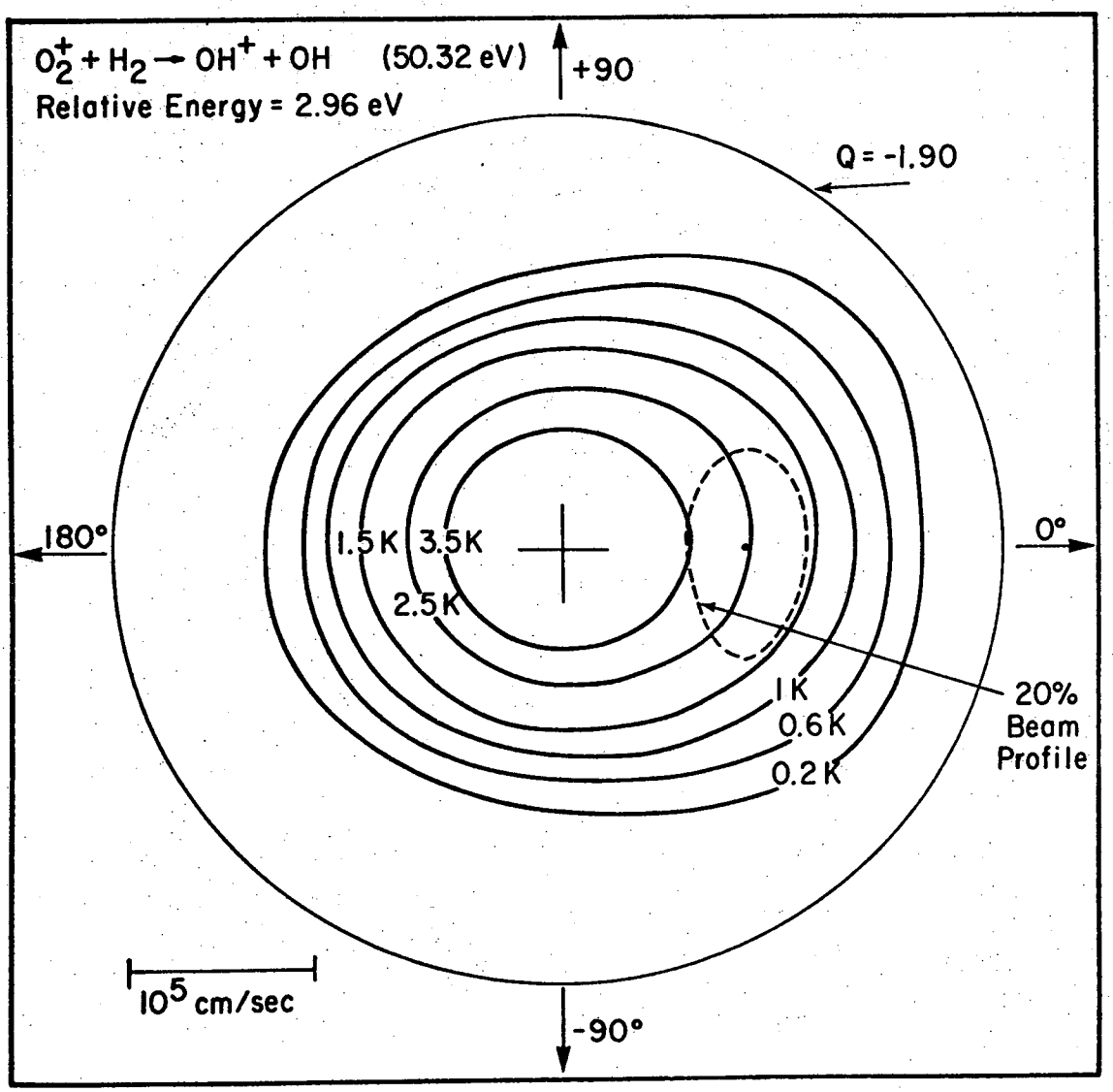

XBL 6912-6700

Fig. 11.

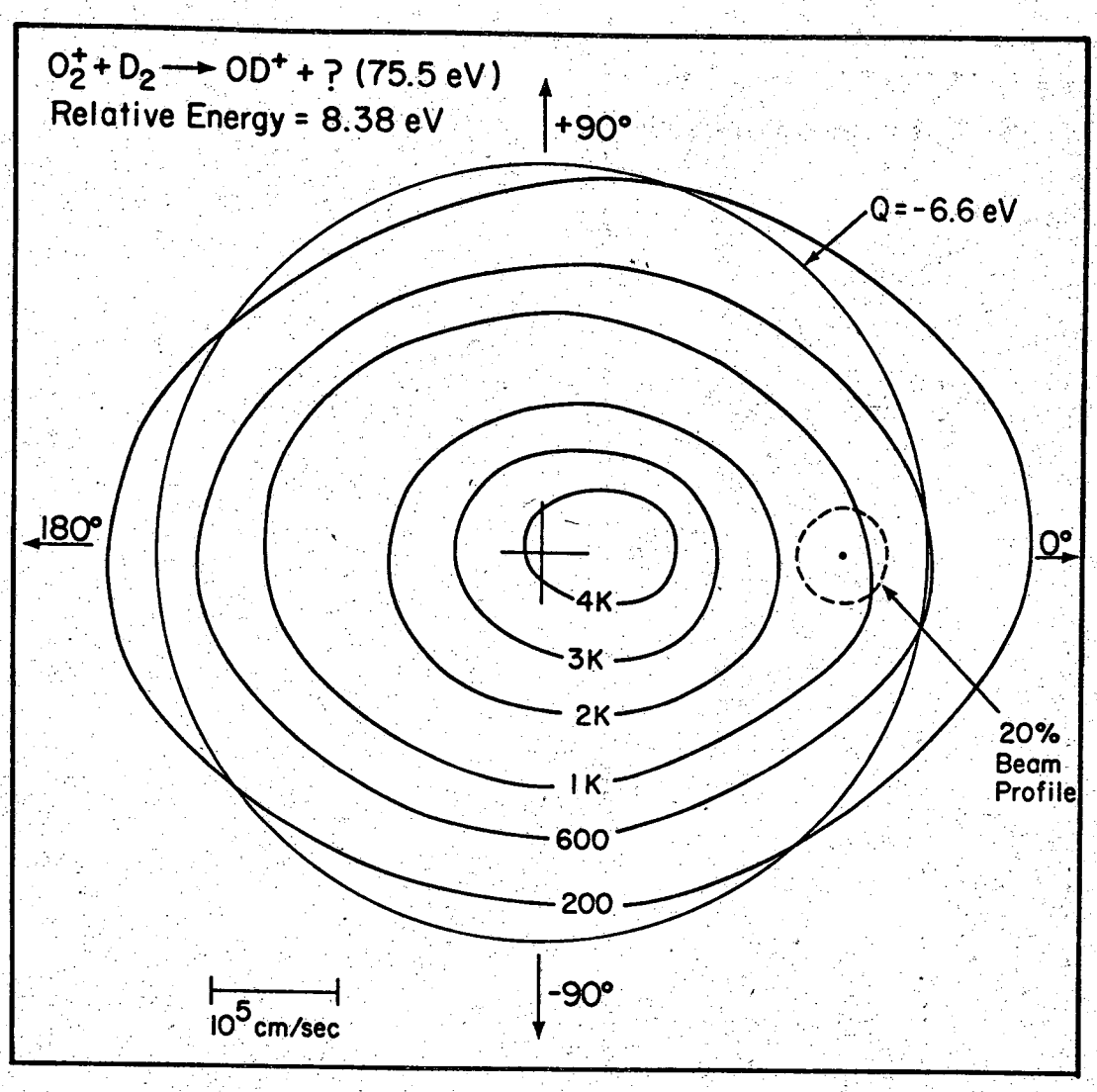

Fig. 12.

XBL 6912-6735

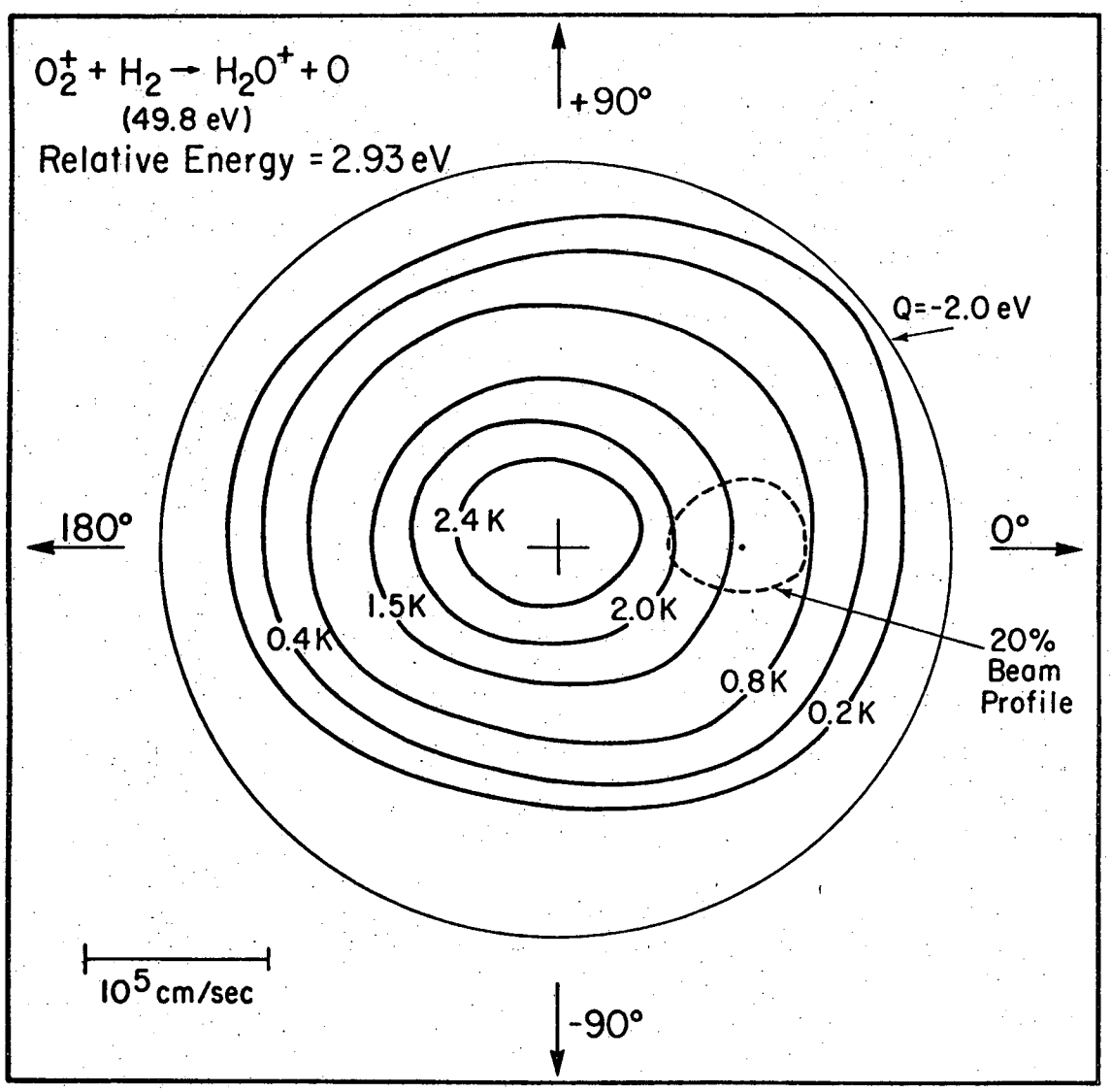

XBL 6912-6694

Fig. 13.

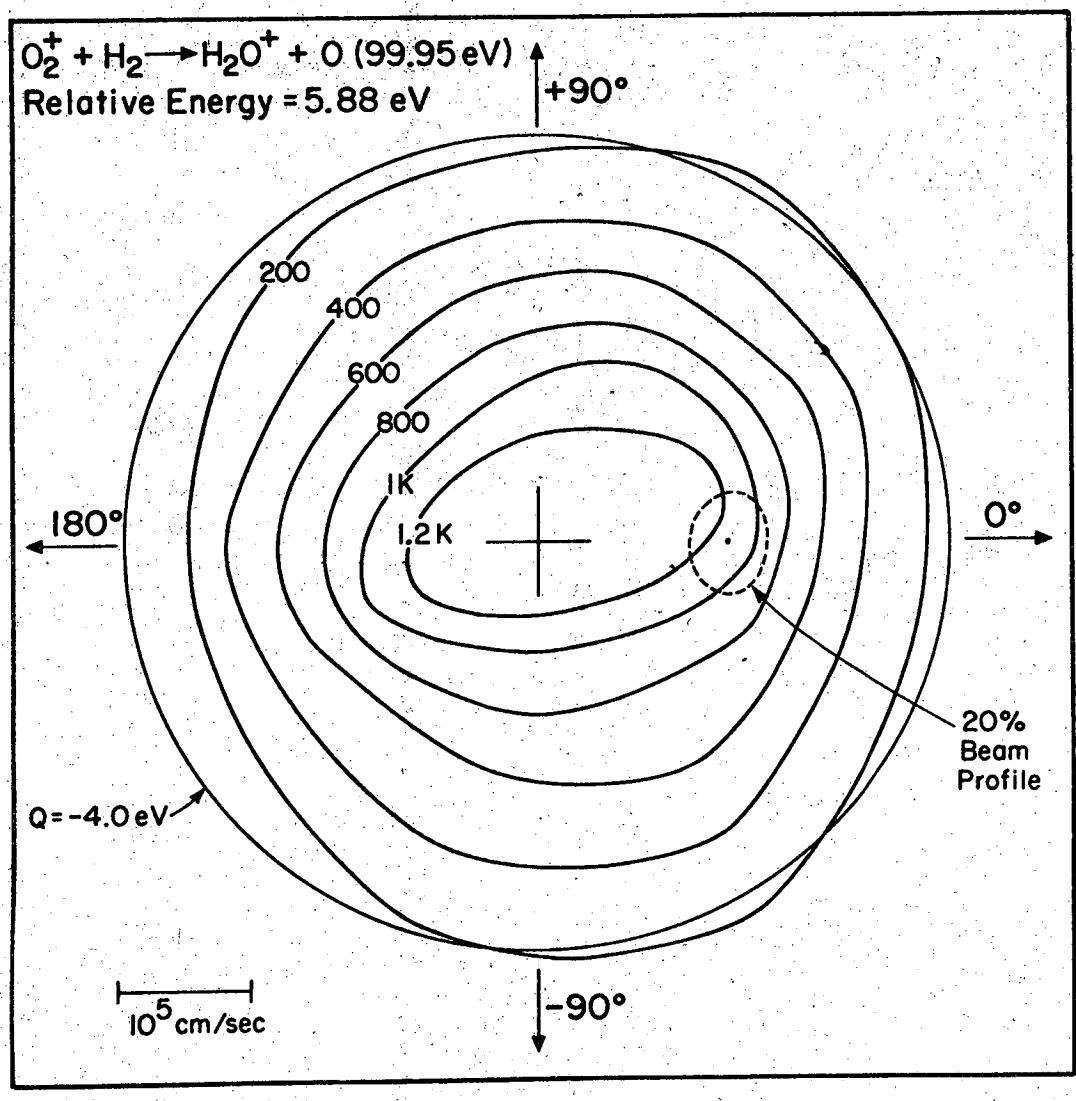
$O_2^+ + H_2 \rightarrow H_2O^+ + O$ (99.95 eV)
Relative Energy = 5.88 eV
+90°
200
400
600
800
1K
1.2K
180°
0°
20% Beam Profile
Q = -4.0 eV
10^5 cm/sec
-90°

Fig. 14.

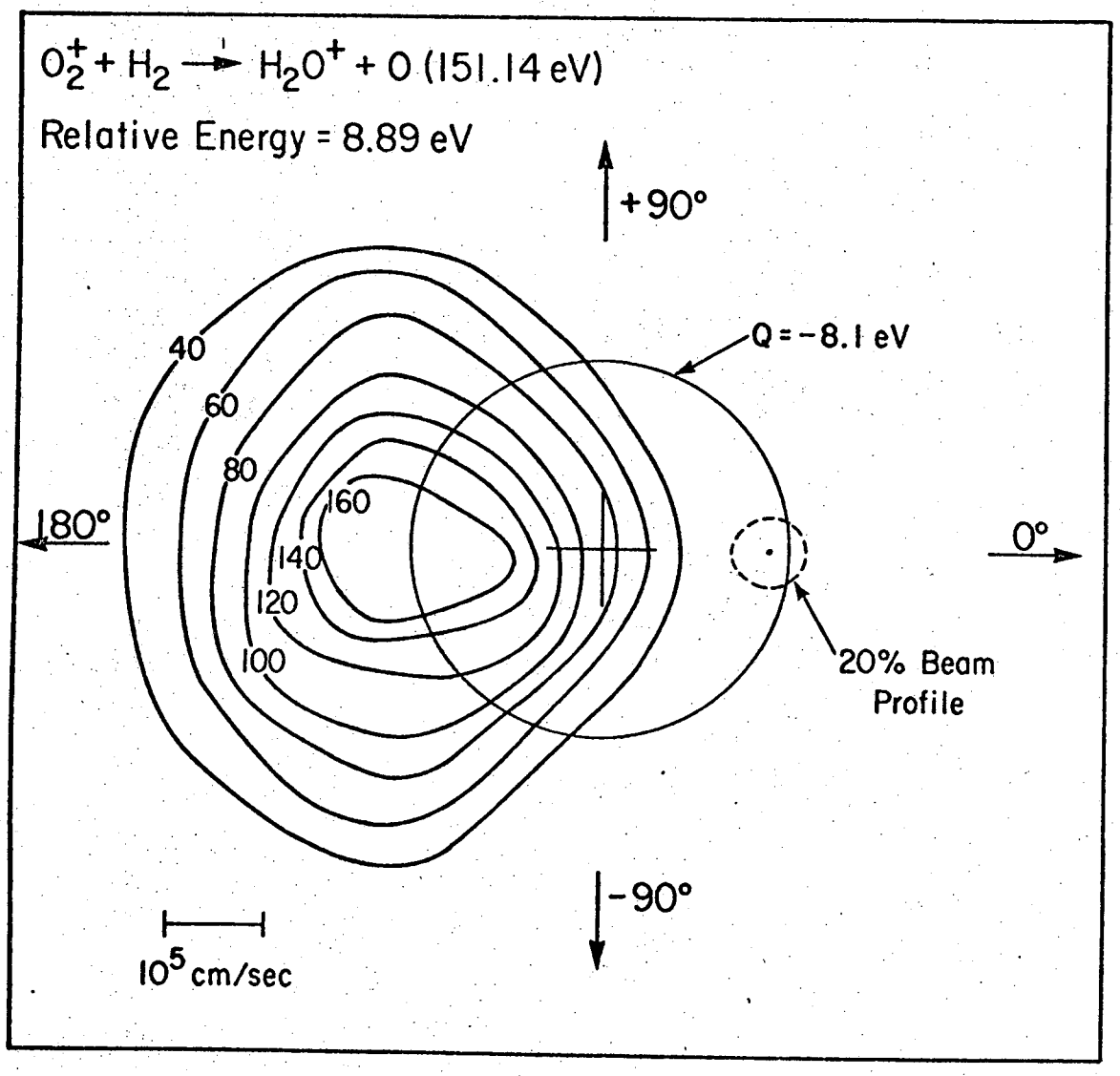
$O_2^+ + H_2 \rightarrow H_2O^+ + O$ (151.14 eV)
Relative Energy = 8.89 eV
+90°
Q = -8.1 eV
40
60
80
160
140
120
100
180°
0°
20% Beam Profile
-90°
10^5 cm/sec

Fig. 15.

LEGAL NOTICE

This report was prepared as an account of work sponsored by the United States Government. Neither the United States nor the United States Atomic Energy Commission, nor any of their employees, nor any of their contractors, subcontractors, or their employees, makes any warranty, express or implied, or assumes any legal liability or responsibility for the accuracy, completeness or usefulness of any information, apparatus, product or process disclosed, or represents that its use would not infringe privately owned rights.

TECHNICAL INFORMATION DIVISION
LAWRENCE RADIATION LABORATORY
UNIVERSITY OF CALIFORNIA
BERKELEY, CALIFORNIA 94720